

---

# Transformer-Based Source-Free Domain Adaptation

---

Guanglei Yang<sup>1</sup> Hao Tang<sup>2</sup> Zhun Zhong<sup>2</sup> Mingli Ding<sup>1</sup> Ling Shao<sup>3</sup> Nicu Sebe<sup>2</sup> Elisa Ricci<sup>1,4</sup>

<sup>1</sup>Haerbin Institute of Technology <sup>2</sup>University of Trento <sup>3</sup>IIAI <sup>4</sup>Fondazione Bruno Kessler

## Abstract

In this paper, we study the task of source-free domain adaptation (SFDA), where the source data are not available during target adaptation. Previous works on SFDA mainly focus on aligning the cross-domain distributions. However, they ignore the generalization ability of the pretrained source model, which largely influences the initial target outputs that are vital to the target adaptation stage. To address this, we make the interesting observation that the model accuracy is highly correlated with whether or not attention is focused on the objects in an image. To this end, we propose a generic and effective framework based on Transformer, named TransDA, for learning a generalized model for SFDA. Specifically, we apply the Transformer as the attention module and inject it into a convolutional network. By doing so, the model is encouraged to turn attention towards the object regions, which can effectively improve the model’s generalization ability on the target domains. Moreover, a novel self-supervised knowledge distillation approach is proposed to adapt the Transformer with target pseudo-labels, thus further encouraging the network to focus on the object regions. Experiments on three domain adaptation tasks, including closed-set, partial-set, and open-set adaptation, demonstrate that TransDA can greatly improve the adaptation accuracy and produce state-of-the-art results. The source code and trained models are available at <https://github.com/ygjwd12345/TransDA>.

## 1 Introduction

Deep learning has enabled several advances in various tasks in computer vision, such as image classification [12, 22], object detection [17, 51], semantic segmentation [38], and so on. However, deep models suffer from significant performance degradation when applied to an unseen target domain, due to the well-documented domain shift problem [18]. To solve this problem, domain adaptation has been introduced, aiming to transfer knowledge from a fully labeled source domain to a target domain [39, 58, 69]. A common strategy in domain adaptation is to align the feature distribution between the source and target domains by minimizing the domain shift through various metrics, such as Correlation Distances [66, 57], Maximum Mean Discrepancy [40, 41, 29], Sliced Wasserstein Discrepancy [32], and Enhanced Transport Distance [33]. Another popular paradigm leverages the idea of adversarial learning [20] to minimize cross-domain discrepancy [64, 34, 56, 54, 31].

Despite the success of current domain adaptation methods, they work under the strict condition that the source data are always available during training. However, such a condition has two drawbacks that hinder the application of these methods. First, the source datasets, such as VisDA [47] and GTAV [52], are usually large and imply high saving and loading costs, restricting their use on certain platforms, especially portable devices. Second, fully accessing the source data may violate data privacy policies. To avoid this issue, companies or organizations prefer to provide the learned models rather than the data. Therefore, designing a domain adaptation method without requiring the source datasets has great practical value. To this end, in this paper, we aim to address the recently introduced problem of source-free domain adaptation [35] (SFDA), in which only the model pretrained on the source and the unlabeled target dataset are provided for target adaptation.

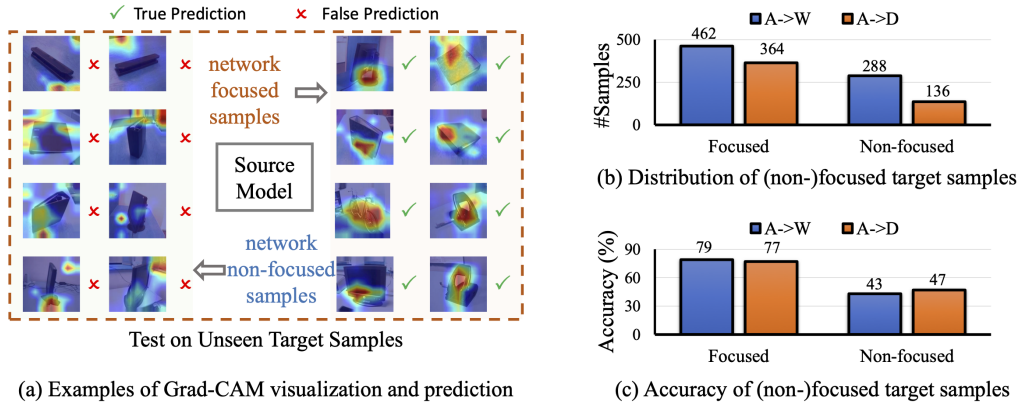


Figure 1: Evaluation of attention for the source model on Office-31 dataset. (a) Examples of Grad-CAM [16] visualization and prediction results in  $A \rightarrow W$ . (b) The distribution and (c) the accuracy of the source model on focused and non-focused samples in  $A \rightarrow W$  and  $A \rightarrow D$ .

So far, few works [34, 35, 1] has been proposed for SFDA, aiming to align the source and target distributions by learning with underlying constraints, such as information maximization and label consistency. However, all of these perform adaptation with a model pretrained on the source data, while neglecting the source model’s generalization ability. In SFDA, the adaptation process largely relies on the accuracy of the source model on the target domain. Without a source model that generalizes well, the generated pseudo-labels may contain significant noise, and learning with them will undoubtedly harm the model’s performance. In this paper, we attempt to improve the generalization ability of the source model for SFDA. Different from existing out-of-domain generalization methods [49, 48], which aims to improve the model generalization by augmenting the diversity of the source samples, in this paper we introduce a new perspective for building a robust source model, motivated by the following observation. In Figure 1, we directly apply the source model on the unseen target samples ( $A \rightarrow W$  and  $A \rightarrow D$  on Office-31 [53]) and produce the heat maps by Grad-CAM [16]. We use Amazon Mechanical Turk and ask annotators to label the samples with “focused / non-focused” according to whether the heat map (red region) is localized on the object. Examples are shown in Figure 1(a). We observe that the accuracy of the focused samples is much higher than that of the non-focused samples (see Figure 1(b, c)). This finding reveals that if a network can effectively focus on the objects in the images, it will have a high prediction accuracy on these images.

Inspired by the above observation, we propose TransDA for SDFDA by equipping a convolutional model with a Transformer [13] module, which can effectively encourage the network to focus on the objects and thus improve the performance on target samples. Specifically, by injecting the Transformer after the last convolutional layer of ResNet-50, we can leverage its long-range dependence to force the model to pay more attention to the objects. Albeit simple, this modification can significantly improve the generalization ability of the source model. In addition, during the target adaptation, we propose a self-supervised knowledge distillation with generated pseudo-labels, further leading the Transformer to learn to focus on the objects of target samples. We evaluate our TransDA on three domain adaptation tasks, including closed-set [53], partial-set [3], and open-set [46] domain adaptation. Extensive results demonstrate that TransDA outperforms state-of-the-art methods on all tasks. For example, on the Office-Home dataset, TransDA advances the best accuracies from 71.8% to **79.3%**, from 79.3% to **81.3%**, and from 72.8% to **76.8%** for the closed-set, partial-set and open-set settings, respectively. To summarize, this work provides the following three contributions:

- Through an in-depth empirical study, we reveal for the first time the importance of the network attention for SFDA. This provides a new perspective for improving the generalization ability of the source model.
- We propose a Transformer-based network for SDFDA, which can effectively lead the model to pay attention to the objects, and thus significantly increases the model generalization ability. To our knowledge, we are the first to propose Transformer for solving the domain adaptation task.
- We introduce a novel self-supervised knowledge distillation approach to further help the Transformer to focus on target objects.

## 2 Related Work

**Traditional Domain Adaptation.** Domain adaptation aims to improve the target learning by using a labeled source domain that belongs to a different distribution. A number of methods have been proposed for unsupervised domain adaptation. One common solution is to guide the model to learn a domain-invariant representation by minimizing the domain discrepancy [66, 57, 40, 41, 29]. For example, ETD [33] employs an enhanced transport distance to reflect the discriminative information. In a similar way, CAN [29] optimizes the network by considering the discrepancy between the intra- and the inter-class domains. More recently, several methods have focused on the feature discrimination ability during domain adaptation. They introduce different normalization or penalization strategies to boost the feature discrimination ability on the target domain, such as batch normalization [6], batch spectral penalization [9], batch nuclear-norm maximization [10], and transferable normalization [62]. Another branch of methods exploit a generative adversarial network to address the domain confusion [15, 58]. BDG [64] and GVB-GD [11] use bi-directional generation to construct domain-invariant representations. Despite the large success of the above methods, they typically require access to source data when learning from the target domain. This may lead to personal information leakage and thus violate data privacy requirements.

**Source-Free Domain Adaptation.** To alleviate the issue of data privacy, recent works [34, 35, 1] have turned their attention to the problem of source-free domain adaptation, where only the pretrained source model and the target samples are provided during the target adaptation stage. C3-GAN [34] introduces a collaborative class conditional generative adversarial net to produce target-style training samples. In addition, a clustering-based regularization is also used to obtain more discriminative features in the target domain. Meanwhile, SHOT [35] freezes the classifier module and learns the target-specific feature extractor with information maximization and self-supervised pseudo-labeling, which can align the target feature distribution with the source domain. DECISION [1] extends SHOT to a multi-source setting by learning different weights for each source model. Different from the above methods, in this paper, we attempt to improve the generalization ability of the source model by injecting a Transformer module into the network. Our approach can be readily incorporated into most existing frameworks to boost the adaptation accuracy.

**Vision Transformers.** The Transformer was first proposed by [59] for machine translation and has been used to establish state-of-the-art results in many natural language processing tasks. Recently, the Vision Transformer (ViT) [13] achieved state-of-the-art results on the image classification task by directly applying Transformers with global self-attention on full-sized images. Since then, Transformer-based approaches have been shown to be efficient in many computer vision tasks, including object detection [5, 72], image segmentation [8, 71], video inpainting [67], virtual try-on [50], video classification [45], pose estimation [26, 27], object re-identification [23], image retrieval [14], and depth estimation [65]. Different from these approaches, in this paper, we adopt a Transformer-based network to tackle the source-free domain adaptation task. To this end, we propose a generic yet straightforward TransDA framework for domain adaptation to encourage the model to focus on the object regions, leading to improved domain generalization.

## 3 Method

### 3.1 Problem Definition

In traditional domain adaptation (DA), models are trained on an unlabeled target domain  $X_t = \{x_t^i\}_{i=1}^M$  and a source domain  $X_s = \{x_s^j\}_{j=1}^N$  along with corresponding labels  $Y_s = \{y_s^j\}_{j=1}^N$ , where  $y_s^j$  belongs to the set of  $K$  classes. The distributions of source and target data are denoted as  $x_s \sim p_{data}(x_s)$  and  $x_t \sim p_{data}(x_t)$ , respectively, where  $p_{data}(x_t) \neq p_{data}(x_s)$ . The goal is to learn a target network  $\phi_t$ , using the labeled source data and unlabeled target data, that can accurately recognize the target samples. In SFDA, (1) the labeled source data is only used to pretrain a source model  $\phi_s$ ; and (2) the target network  $\phi_t$  is learned with the pretrained source model  $\phi_s$  and the unlabeled target data  $X_t$ .

### 3.2 Overview

The overall framework of the proposed method, which consists of (1) source training and (2) target adaptation, is shown in Figure 2. First, we train the source model  $\phi_s$  with samples from the source domain using the cross-entropy loss. The source model  $\phi_s$  is composed of two modules: the feature

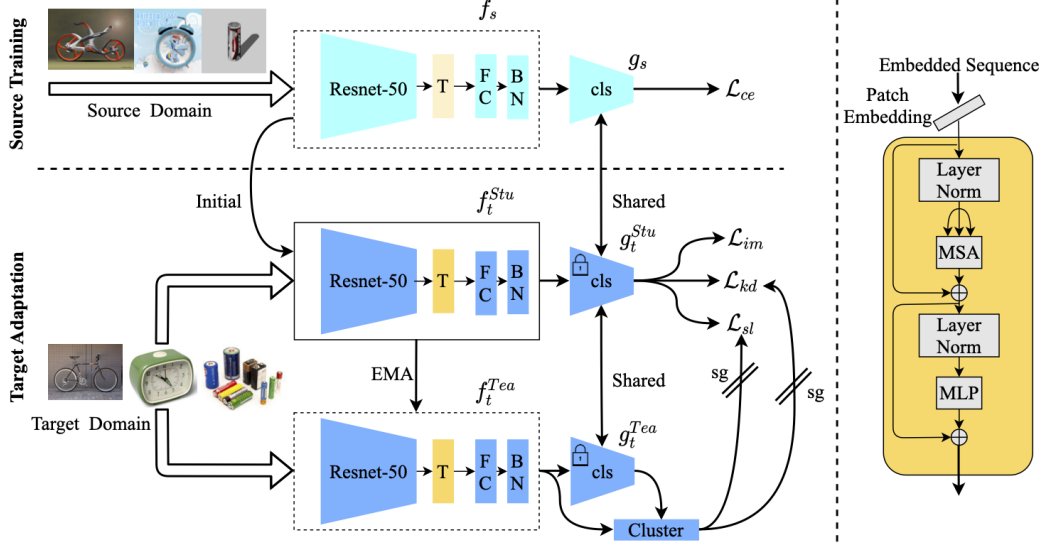


Figure 2: Overview of the proposed method. The model includes a feature extractor  $f$  and a classifier  $g$ . We inject a Transformer module (structure is shown on the right) into  $f$  to obtain a representation with improved generalization capability. First, we train the model with the labeled source data. Then, we create a teacher model ( $Tea$ ) and a student ( $Stu$ ), cloned from the source model, for target adaptation. The teacher model is used to produce pseudo-labels for computing the self-labeling loss ( $\mathcal{L}_{sl}$ ) and knowledge distillation loss ( $\mathcal{L}_{kd}$ ). We also calculate the information maximization loss ( $\mathcal{L}_{im}$ ) based on the outputs of the student model. Here,  $sg$ : stop-gradient,  $EMA$ : exponential moving average,  $FC$ : fully connected layer,  $BN$ : batch normalization layer.

extractor  $f_s: \mathcal{X} \rightarrow \mathcal{R}^d$  and the classifier  $g_s: \mathcal{R}^d \rightarrow \mathcal{R}^K$ , where  $d$  indicates the dimension of the output of the feature extractor and  $K$  refers to the number of categories in the source data. Therefore, we have  $\phi_s = f_s \circ g_s$ . Different from existing methods that use a convolutional neural network (CNN) as the feature extractor (e.g., ResNet [22]), we propose to inject a Transformer module [13] after the last layer of the CNN, which can help the feature extractor pay more attention to the objects and thus produce a more robust representation. Second, we aim to learn a network  $\phi_t$  in the target domain, given the pretrained  $\phi_s$ . Specifically, we maintain a teacher model  $\phi_t^{Tea}$  and a student model  $\phi_t^{Stu}$ , which are both initialized by the parameters of  $\phi_s$ . Following [35], we fix the classifiers and only update the feature extractors. The updating strategies for the feature extractors are different. For  $f_t^{Stu}$ , we update it with the gradients produced by the target adaptation losses.  $f_t^{Tea}$  is updated with an exponential moving average of the parameters of  $f_t^{Stu}$ . The teacher model  $\phi_t^{Tea}$  is used to produce a hard pseudo-label  $\hat{y}_t$  and soft pseudo-label  $\bar{y}_t$  for calculating the self-labeling loss and knowledge distillation loss, respectively. In addition, the information maximization loss is computed with the outputs of  $\phi_t^{Stu}$ . The above three losses are used to update  $f_t^{Stu}$ , where the information maximization and self-labeling losses are employed to align the cross-domain feature distributions and the knowledge distillation loss is designed to force the model to focus on objects.

### 3.3 Model Pretraining on Source with Transformer

**Loss Function.** In this stage, we aim to learn a source model with the labeled source data. Generally, given a network  $\phi_s$  initialized on ImageNet [12], we train it with the label smoothing cross-entropy loss [44]:

$$\mathcal{L}_{ce} = -\mathbb{E}_{x_s \in X_s} \sum_{k=1}^K \hat{y}_k \log \sigma(\phi_s(x_s)), \quad (1)$$

where  $\hat{y}_k = (1 - \alpha) y_k + \alpha/K$ .  $\alpha$  is the smoothing factor and is empirically set to 0.1.  $\sigma(\cdot)$  is the softmax operation.

**Discussion.** In SFDA, the target adaptation stage greatly relies on the target outputs obtained by the source model. Hence, it is important to learn a robust source model, such as to counteract with domain bias. As shown in Figure 1, the model can effectively classify the target samples if it can

localize the object regions. This observation is reasonable, because the model learns to capture the common object patterns instead of domain-specific information (*e.g.*, background, color distribution) if it can always focus on the objects. Therefore, one solution for improving the generalization ability is forcing the model to focus on objects during training. Existing approaches typically select a CNN model as the feature extractor of  $\phi_s$ . However, due to the intrinsic locality of the convolution operation (*i.e.*, small receptive fields), the CNN model prefers to capture local information, which may lead it to overfit on domain-specific information and thus fail to focus on objects, especially when encountering a large domain shift.

**Equipping the Model with a Transformer.** To address the drawback of CNNs in SFDA, in this paper, we propose to inject a Transformer module after the convolutional network [13]. By doing so, we can leverage the property of the Transformer to capture long-range dependencies and explicitly encourage the model pay more attention to the objects. This enables us to reduce the impact of domain-specific information and produce more robust and transferable representations.

Specifically, we construct the feature extractor by injecting the Transformer after the last convolutional layer of ResNet-50 [22]. Since the input of the transformer should be a sequence, we first reshape the output of the ResNet-50 backbone  $F \in \mathcal{R}^{h \times w \times \hat{d}}$  to  $\hat{F} \in \mathcal{R}^{u \times \hat{d}}$ , where  $h$ ,  $w$ , and  $\hat{d}$  indicate the height, width, and dimension of  $F$ , respectively.  $u$  is the product of  $h$  and  $w$ . Then,  $\hat{F}$  is regarded as the input sequence with patch embeddings for the Transformer.

In the first layer of the Transformer, we map the dimension of the patch embeddings  $\hat{F}$  from  $\hat{d}$  to  $\bar{d}$  with a linear projection layer, producing  $Z_0 \in \mathcal{R}^{u \times \bar{d}}$ . Then,  $Z_0$  is fed into  $L$  Transformer layers, which include multi-headed self-attention (MSA) and multi-layer perceptron (MLP) blocks.

Given the feature  $Z_{l-1}$  obtained from the  $l-1$ -th Transformer layer, MSA ( $Z_{l-1}$ ) is defined as:

$$\text{MSA}(Z_{l-1}) = Z_{l-1} + \text{cont}(\text{AH}_1(\text{LN}(Z_{l-1})); \text{AH}_2(\text{LN}(Z_{l-1})); \dots; \text{AH}_m(\text{LN}(Z_{l-1}))) \times W, \quad (2)$$

where AH represents a self-attention head [59],  $\text{cont}(\cdot)$  is the concentration operation,  $\text{LN}(\cdot)$  is the layer normalization [61], and  $m$  indicates the number of self-attention heads.  $W \in \mathbb{R}^{m \cdot \bar{d} \times \bar{d}}$  are the learnable weight matrices, where  $\bar{d}$  is the output dimension of each AH.

The output of MSA is then transformed into an MLP block with a residual skip, formulated as:

$$Z_l = \text{MLP}(\text{LN}(\text{MSA}(Z_{l-1}))) + \text{MSA}(Z_{l-1}). \quad (3)$$

The structure of the Transformer layer is illustrated in the right part of Figure 2.

Given the output  $Z_l \in \mathcal{R}^{u \times \bar{d}}$  of the Transformer, we obtain the global feature by average pooling, which is fed into the following layers, including one FC layer, one BN layer, and the classifier  $g_s$ .

### 3.4 Self-Training on Target with Transformer

**Information Maximization.** In the target adaptation stage, we are given a pretrained source model  $\phi_s$  and the unlabeled target domain. We first initialize the target model  $\phi_t$  with the parameters of  $\phi_s$ . Following [35], we fix the classifier  $g_t$  to maintain the class distribution information of the source domain, and update the feature extractor  $f_t$  using the information maximization (IM) loss [2, 19, 25]. This enables us to reduce the feature distribution gap between the source and target domains. The IM loss consists of a conditional entropy term and a diversity term:

$$\mathcal{L}_{im} = -\mathbb{E}_{x_t \in X_t} \sum_{k=1}^K \sigma(\phi_t(x_t)) \log \sigma(\phi_t(x_t)) + \sum_{k=1}^K \bar{p}_k \log \bar{p}_k, \quad (4)$$

where  $\bar{p} = \mathbb{E}_{x_t \in X_t} [\sigma(\phi_t(x_t))]$  is the mean of the softmax outputs for the current batch.

**Self-Labeling.** Although the IM loss can make the predictions on the target domain more confident and globally diverse, it is inevitably affected by the noise generated by wrong label matching. To address this issue, one solution is to utilize a self-labeling strategy to further constrain the model. In this paper, we use self-supervised clustering [35, 1, 34] to generate pseudo-labels for target samples. Specifically, we first compute the centroid for each class in the target domain by weighted k-means clustering,

$$\mu_k^{(0)} = \frac{\sum_{x_t \in X_t} \sigma(\phi_t(x_t)) f_t(x_t)}{\sum_{x_t \in X_t} \sigma(\phi_t(x_t))}. \quad (5)$$

Then, the initial pseudo-labels are generated by the nearest centroid classifier:

$$\hat{y}_t = \arg \min_k 1 - \frac{f_t(x_t) \cdot \mu_k^{(0)}}{\|f_t(x_t)\|_2 \|\mu_k^{(0)}\|_2}, \quad (6)$$

where  $\|*\|_2$  denotes the  $L2$ -norm. Finally, the class centroids and pseudo-labels are updated as follows:

$$\mu_k^{(1)} = \frac{\sum_{x_t \in X_t} \xi(\hat{y}_t = k) f_t(x_t)}{\sum_{x_t \in X_t} \xi(\hat{y}_t)}, \quad \hat{y}_t = \arg \min_k 1 - \frac{f_t(x_t) \cdot \mu_k^{(1)}}{\|f_t(x_t)\|_2 \|\mu_k^{(1)}\|_2}, \quad (7)$$

where  $\xi(*)$  is an indicator that produces 1 when the argument is true. Although the pseudo-labels and the centroids can be updated by Eq. (7) multiple times, we find that one round of updating is sufficient. Given the generated pseudo-labels, the loss function for self-labeling is calculated using the cross-entropy loss, formulated by:

$$\mathcal{L}_{sl} = -\mathbb{E}_{x_t \in X_t} \sum_{k=1}^K \xi(\hat{y}_t = k) \log \sigma(\phi_t(x_t)). \quad (8)$$

**Self-Knowledge Distillation.** Recall that we aim to encourage the network to focus on the objects in order to produce more robust feature representations. Although we inject a Transformer module into the model to achieve this goal, we hope to further improve object attention ability by learning with the target samples. The above loss functions ( $\mathcal{L}_{im}$  and  $\mathcal{L}_{sl}$ ) are designed to align the feature distribution of the domain, but do not explicitly consider the attention constraint. Therefore, they cannot further improve object attention ability of the Transformer. DINO [7] showed that learning with a self-knowledge distillation strategy can lead the Transformer to capture more semantic information, *i.e.*, pay more attention to objects. Inspired by this observation, we propose to adopt the self-knowledge distillation strategy to force the model to turn more attention to objects in the target samples.

Specifically, we employ a teacher model  $\phi_t^{Tea}$  and a student model  $\phi_t^{Stu}$  to implement self-knowledge distillation. We use the teacher model  $\phi_t^{Tea}$  to generate pseudo-labels and optimize the parameters of the student model  $\phi_t^{Stu}$  with training losses. Hence, Eq. (5), Eq. (6), and Eq. (7) are re-formulated by replacing  $f_t$  and  $g_t$  with  $f_t^{Tea}$  and  $g_t^{Tea}$ , respectively. Similarly,  $\mathcal{L}_{im}$  and  $\mathcal{L}_{sl}$  are re-formulated by replacing  $\phi_t$  with  $\phi_t^{Stu}$ .

For the self-knowledge distillation, we generate the soft pseudo-labels by

$$\bar{y}_t = \frac{\exp(\delta(f_t^{Tea}(x_t), \mu_k^{(1)})/\tau)}{\sum_{k=1}^K \exp(\delta(f_t^{Tea}(x_t), \mu_k^{(1)})/\tau)}, \quad (9)$$

where  $\delta(a, b)$  indicates the cosine distance between  $a$  and  $b$ . Then, our knowledge distillation loss is formulated as:

$$\mathcal{L}_{kd} = -\mathbb{E}_{x_t \in X_t} \sum_{k=1}^K \bar{y}_t \log \phi_t^{Stu}(x_t). \quad (10)$$

In summary, the final objective of self-training on the target domain is given by

$$\mathcal{L}_{tgt} = \mathcal{L}_{im} + \alpha \mathcal{L}_{sl} + \beta \mathcal{L}_{kd}, \quad (11)$$

where  $\alpha$  and  $\beta$  are the weights of self-labeling loss and self-knowledge distillation loss. We update  $\phi_t^{Stu}$  with  $\mathcal{L}_{tgt}$ . Meanwhile, we update  $\phi_t^{Tea}$  with an exponential moving average of the parameters of  $\phi_t^{Stu}$ . Note that the classifiers of  $\phi_t^{Tea}$  and  $\phi_t^{Stu}$  are both fixed during training.

## 4 Experiments

### 4.1 Experimental Setup

**Datasets.** We conduct experiments on three datasets, including Office-31 [53], Office-Home [60], and VisDA [47]. Office-31 includes 4,652 images and 31 categories from three domains, *i.e.*, Amazon (A), Webcam (W), and DSLR (D). Office-Home consists of around 15,500 images from 65 categories. It is

Table 1: Accuracy (%) on Office-31 for closed-set domain adaptation (ResNet-50).

Method	A→D	A→W	D→W	W→D	D→A	W→A	Avg
ETD [33]	88.0	92.1	<b>100.0</b>	<b>100.0</b>	71.0	67.8	86.2
BDG [64]	93.6	93.6	99.0	<b>100.0</b>	73.2	72.0	88.5
CDAN+BSP [9]	93.0	93.3	98.7	<b>100.0</b>	73.6	72.6	88.5
CDAN+BNM [10]	92.9	92.8	98.8	<b>100.0</b>	73.5	73.8	88.6
CDAN+TransNorm [62]	94.0	<b>95.7</b>	98.7	<b>100.0</b>	73.4	74.2	89.3
GVB-GD [11]	96.1	93.8	98.8	<b>100.0</b>	74.9	72.8	89.4
GSDA [24]	94.8	<b>95.7</b>	99.1	<b>100.0</b>	73.5	74.9	89.7
SHOT [35]	94.0	90.1	98.4	99.9	74.7	74.3	88.6
3C-GAN [34]	92.7	93.7	98.5	99.8	75.3	77.8	89.6
CAN [29]	95.0	94.5	99.1	99.8	<b>78.0</b>	77.0	90.6
TransDA (Ours)	<b>97.2</b>	95.0	99.3	99.6	73.7	<b>79.3</b>	<b>90.7</b>

Table 2: Accuracy (%) on Office-Home for closed-set domain adaptation (ResNet-50).

Method	Ar→Cl	Ar→Pr	Ar→Rw	Cl→Ar	Cl→Pr	Cl→Rw	Pr→Ar	Pr→Cl	Pr→Rw	Rw→Ar	Rw→Cl	Rw→Pr	Avg
ETD [33]	51.3	71.9	85.7	57.6	69.2	73.7	57.8	51.2	79.3	70.2	57.5	82.1	67.3
BDG [64]	51.5	73.4	78.7	65.3	71.5	73.7	65.1	49.7	81.1	74.6	55.1	84.8	68.7
CDAN+BNM [10]	56.2	73.7	79.0	63.1	73.6	74.0	62.4	54.8	80.7	72.4	58.9	83.5	69.4
CDAN+TransNorm [62]	56.3	74.2	79.0	63.9	73.5	73.1	62.3	55.2	80.3	73.5	58.4	83.3	69.4
GVB-GD [11]	57.0	74.7	79.8	64.6	74.1	74.6	65.2	55.1	81.0	74.6	59.7	84.3	70.4
GSDA [24]	61.3	76.1	79.4	65.4	73.3	74.3	65.0	53.2	80.0	72.2	60.6	83.1	70.3
RSDA+DANN [21]	53.2	77.7	81.3	66.4	74.0	76.5	67.9	53.0	82.0	75.8	57.8	85.4	70.9
SHOT [35]	57.1	78.1	81.5	68.0	78.2	78.1	67.4	54.9	82.2	73.3	58.8	84.3	71.8
TransDA (Ours)	<b>67.5</b>	<b>83.3</b>	<b>85.9</b>	<b>74.0</b>	<b>83.8</b>	<b>84.4</b>	<b>77.0</b>	<b>68.0</b>	<b>87.0</b>	<b>80.5</b>	<b>69.9</b>	<b>90.0</b>	<b>79.3</b>

composed of four domains: Artistic images (Ar), Clip Art (Cl), Product images (Pr), and Real-World images (Rw). VisDA contains 152K synthetic images (regarded as the source domain) and 55K real object images (regarded as the target domain), which are divided into 12 shared classes.

**Evaluation Settings.** We evaluate the proposed method on three DA settings, including closed-set DA, partial-set DA [4], and open-set DA [37]. Closed-set DA is a standard setting, which assumes that the source and target domains share the same class set. Partial-set DA assumes that the target domain belongs to a sub-class set of the source domain. In contrast, open-set DA assumes that the target domain includes unknown classes that are absent in the source domain. For closed-set DA, we evaluate our method on all three datasets. For partial-set and open-set DA, we evaluate our method on Office-Home. Following [35], for partial-set DA, we choose 25 classes for the target domain, while all 65 classes are used for the source domain. For open-set DA, we select 25 classes as the shared classes while the other classes make up the unknown class in the target domain.

**Implementation Details.** We use a ResNet-50 [22] pretrained on ImageNet [22] as the feature extractor backbone. Moreover, the Transformer [13] layers are injected after the backbone, followed by a bottleneck layer with batch normalization [28] and a task-specific classifier layer. Different from [35, 1], we adopt a teacher-student structure for target adaptation. We use stochastic gradient descent (SGD) with momentum 0.9 and weight decay  $10^{-3}$  to update the network. The learning rates are set to  $10^{-3}$  for the backbone and Transformer layers and set to  $10^{-2}$  for the bottleneck and classifier layers. For source training, we train the model over 100, 50, and 10 epochs for Office-31, Office-Home, and VisDA, respectively. For target adaptation, the number of epochs is set to 15 for all settings. We set  $\alpha$  and  $\beta$  in Eq. (11) to 0.3 and 1, respectively, which yields consistently high performance across all settings. The batch size is set to 64, and the size of the input image is reshaped to  $224 \times 224$ .

## 4.2 Comparison with State-of-the-Art Methods

We first compare the proposed TransDA with state-of-the-art methods under the closed-set, partial-set, and open-set DA. For closed-set DA, the compared methods include: ETD [33], BDG [64], BSP [9], BNM [10], TransNorm [62], GVB-GD [11], GSDA [24], CAN [29], SHOT [35], GSDA [24], RSDA [21], DANN [15], CDAN [42], MDD [70], and 3C-GAN [34]. For partial-set DA and open-set DA, we compare with ETN [4], SAFN [63], SHOT [35], TIM [30], OSBP [55], STA [37], and BA<sup>3</sup>US [36]. In these methods, only SHOT [35] and 3C-GAN [34] are designed for source-free domain adaptation.

**Results on Closed-Set DA.** We report the results on Office-31, Office-Home, and VisDA in Table 1, Table 2, and Table 3, respectively. We can make the following three observations. (1) Our TransDA outperforms all compared methods on all datasets, yielding state-of-the-art accuracies for closed-set DA. (2) When using the same backbone, our TransDA surpasses the source-free method (SHOT [35]) by a large margin. Specifically, when using ResNet-50 as the backbone, TransDA outperforms SHOT [35] by 2.1%, 7.5%, and 8.0% on Office-31, Office-Home, and VisDA, respectively. This

Table 3: Accuracy (%) on VisDA for closed-set domain adaptation (ResNet-50). \* indicates the methods that use ResNet-101 as the backbone. † indicates reproduction using the official code.

Method	airplane	bicycle	bus	car	horse	knife	motorcycle	person	plant	skateboard	train	truck	Avg
DANN [15]	-	-	-	-	-	-	-	-	-	-	-	-	63.7
CDAN [42]	-	-	-	-	-	-	-	-	-	-	-	-	70.0
MDD [70]	-	-	-	-	-	-	-	-	-	-	-	-	74.6
RSDA [21]	-	-	-	-	-	-	-	-	-	-	-	-	75.8
GSDA [24]	93.1	67.8	83.1	<b>83.4</b>	94.7	93.4	93.4	79.5	93.0	88.8	83.4	36.7	81.5
SHOT [35]†	94.5	85.7	77.3	52.2	91.6	15.7	82.6	80.3	87.8	88.0	85.1	58.8	75.0
TransDA (Ours)	<b>97.2</b>	<b>91.1</b>	81.0	57.5	<b>95.3</b>	93.3	82.7	67.2	92.0	<b>91.8</b>	<b>92.5</b>	<b>54.7</b>	<b>83.0</b>
SWD [32]*	90.8	82.5	81.7	70.5	91.7	69.5	86.3	77.5	87.4	63.6	85.6	29.2	76.4
3C-GAN [34]*	94.8	73.4	68.8	74.8	93.1	<b>95.4</b>	88.6	<b>84.7</b>	89.1	84.7	83.5	48.1	81.6
STAR [43]*	95.0	84.0	<b>84.6</b>	73.0	91.6	91.8	85.9	78.4	<b>94.4</b>	84.7	87.0	42.2	82.7
SHOT [35]*	94.3	88.5	80.1	57.3	93.1	94.9	80.7	80.3	91.5	89.1	86.3	58.2	82.9

Table 4: Accuracy (%) on Office-Home for partial-set and open-set domain adaptation (ResNet-50).

Partial-set DA	Ar→Cl	Ar→Pr	Ar→Rw	Cl→Ar	Cl→Pr	Cl→Rw	P→Ar	Pr→Cl	Pr→Rw	Rw→Ar	Rw→Cl	Rw→Pr	Avg
IWAN [68]	53.9	54.5	78.1	61.3	48.0	63.3	54.2	52.0	81.3	76.5	56.8	82.9	63.6
SAN [3]	44.4	68.7	74.6	67.5	65.0	77.8	59.8	44.7	80.1	72.2	50.2	78.7	65.3
ETN [4]	59.2	77.0	79.5	62.9	65.7	75.0	68.3	55.4	84.4	75.7	57.7	84.5	70.5
SAFN [63]	58.9	76.3	81.4	70.4	73.0	77.8	72.4	55.3	80.4	75.8	60.4	79.9	71.8
BA <sup>3</sup> US [36]	60.6	83.2	88.4	71.8	72.8	83.4	75.5	61.6	86.5	79.3	62.8	86.1	76.0
SHOT [35]	64.8	<b>85.2</b>	<b>92.7</b>	<b>76.3</b>	77.6	<b>88.8</b>	79.7	64.3	<b>89.5</b>	80.6	66.4	85.8	79.3
TransDA (Ours)	<b>73.0</b>	79.5	90.9	72.0	<b>83.4</b>	86.0	<b>81.1</b>	<b>71.0</b>	86.9	<b>87.8</b>	<b>74.9</b>	<b>89.2</b>	<b>81.3</b>
Open-set DA	Ar→Cl	Ar→Pr	Ar→	Cl→Ar	Cl→Pr	Cl→Rw	Pr→Ar	Pr→Cl	Pr→Rw	Rw→Ar	Rw→Cl	Rw→Pr	Avg
ATI-A [46]	55.2	52.6	53.5	69.1	63.5	74.1	61.7	64.5	70.7	79.2	72.9	75.8	66.1
OSBP [55]	56.7	51.5	49.2	67.5	65.5	74.0	62.5	64.8	69.3	80.6	74.7	71.5	65.7
STA [37]	58.1	53.1	54.4	<b>71.6</b>	69.3	81.9	63.4	65.2	74.9	<b>85.0</b>	<b>75.8</b>	80.8	69.5
TIM [30]	60.1	54.2	56.2	70.9	70.0	78.6	64.0	66.1	74.9	83.2	75.7	81.3	69.6
SHOT [35]	64.5	<b>80.4</b>	<b>84.7</b>	63.1	75.4	81.2	65.3	59.3	<b>83.3</b>	69.6	64.6	82.3	72.8
TransDA (Ours)	<b>71.9</b>	79.1	84.3	71.4	<b>77.1</b>	<b>82.0</b>	<b>68.2</b>	<b>67.5</b>	83.1	76.0	73.0	<b>87.6</b>	<b>76.8</b>

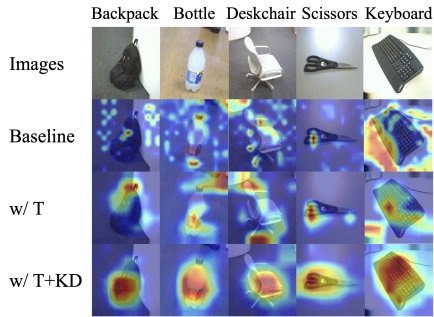
verifies the effectiveness of the proposed TransDA for source-free DA. (3) On VisDA, TransDA with ResNet-50 can produce competitive results compared to the methods that use ResNet-101 as the backbone, further demonstrating the superiority of the proposed TransDA .

**Results on Partial-Set and Open-Set DA.** To verify the versatility of TransDA , we evaluate it on two more challenging tasks, *i.e.*, partial-set DA and open-set DA. Results on Office-Home are reported in Table 4. The advantage of TransDA is similar to that for closed-set DA. That is, TransDA clearly outperforms the compared methods on both settings. Specifically, TransDA is 2.0% and 4.0% better than SHOT [35] on partial-set DA and open-set DA, respectively. This demonstrates that our Transformer-based structure is effective under various domain adaptation settings.

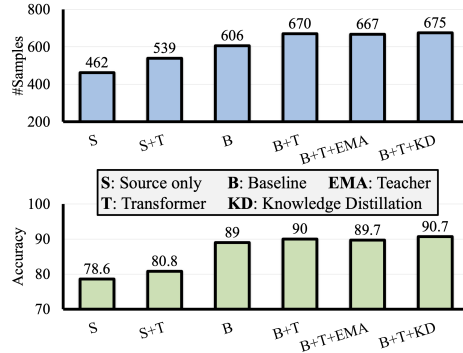
### 4.3 Ablation Study

**Accuracy Comparison.** In Table 5, we study the effectiveness of the proposed Transformer structure and self-knowledge distillation. We first explain the components in Table 5: *Source Only* indicates the pretrained source model; *Baseline* denotes further training the model on the target data with the information maximization and self-labeling losses; *+Transformer* means injecting the Transformer module into the model; *+EMA* refers to using the teacher-student structure; and *+KD* indicates using the self-knowledge distillation loss. From Table 5, we can draw the following conclusions. (1) Injecting the Transformer into the network can consistently improve the results, regardless the model as learnt on the source data or the target data. Specifically, when using the Transformer, the accuracy of *Baseline* improves from 72.1% to 78.8% on Office-Home. This demonstrates the effectiveness of the Transformer in domain adaptation. (2) Adding the knowledge distillation loss can further boost the performance, verifying the advantage of the self-knowledge distillation. (3) Applying the teacher-student structure fails to produce clear improvements, indicating that the gains of *+KD* are mainly obtained by the knowledge distillation rather than by generating pseudo-labels with the teacher model.

**Visualization of Grad-CAM and Statistics Study for Focused and Non-Focused Samples.** In Figure 3(a), we compare the Grad-CAM visualizations for different variants of our method. We obtain the following findings. (1) When adding the Transformer into the network, the red regions on the objects increase, indicating that the network is encouraged to pay more attentions on the objects. (2) When training the model with the knowledge distillation loss, the attention ability of the network is further improved. In addition, we use Amazon Mechanical Turk to estimate the “focused / non-focused” samples for different methods (Figure 3(b)). We can observe that the focused samples



(a) Grad-CAM visualization



(b) Comparisons of focused samples and accuracy

Figure 3: Visualization of (a) Grad-CAM and (b) statistics studies for different methods. Results are evaluated on Office-31 (A→C).

Table 5: Ablation study on the Transformer, teacher-student structure (EMA) and self-knowledge distillation (KD). Results are evaluated for the closed-set DA under Office-31, Office-Home, and VisDA.

Method	Office-31	Office-Home	VisDA
Source Only	78.6	65.7	46.7
+ Transformer	<b>80.8</b>	<b>67.6</b>	<b>48.0</b>
Baseline	89.0	72.1	75.0
+ Transformer	90.0	78.8	81.0
+ Transformer + EMA	90.2	78.7	81.2
+ Transformer + KD	<b>90.7</b>	<b>79.3</b>	<b>83.0</b>

and accuracies increase when adding the Transformer and the knowledge distillation loss. The above observations verify that 1) the proposed Transformer structure and knowledge distillation loss can effectively encourage the network to focus on objects, and 2) improving the attention ability of the network can consistently improve the accuracy for domain adaptation.

**t-SNE Visualization.** In Figure 4, we show the t-SNE of features for different methods. We find that adding the Transformer and the knowledge distillation can (1) lead the intra-class samples to be more compact and (2) reduce the distances between source and target domains clusters. These findings reveal that TransDA can encourage the model to be more robust to intra-class variations and can decrease the cross-domain distribution gap.

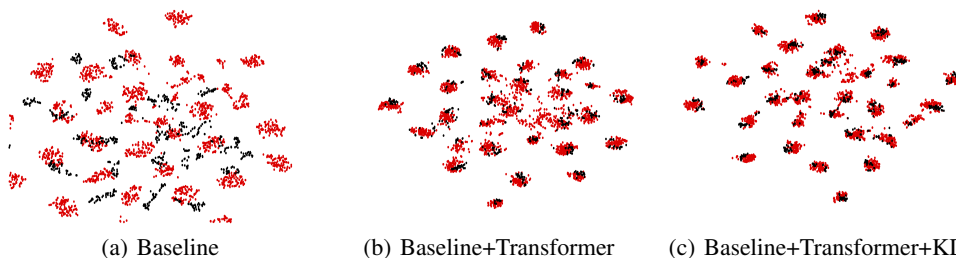


Figure 4: t-SNE visualization for different methods on Office-31 (A→W). We use the outputs of the feature extractor as the features. Red/black denote the source/target domains. Best viewed in color.

## 5 Conclusion

In this paper, we propose a generic yet straightforward representation learning framework, named TransDA, for source-free domain adaptation (SFDA). Specifically, by employing a Transformer module and learning the model with the self-knowledge distillation loss, the network is encouraged to pay more attention to the objects in an image. Experiments on closed-set, partial-set, and open-set DA confirm the effectiveness of the proposed TransDA. Importantly, this work reveals that the attention ability of a network is highly related to its adaptation accuracy. We hope these findings will provide a new perspective for designing domain adaptation algorithms in the future.

## References

- [1] Sk Miraj Ahmed, Dripta S Raychaudhuri, Sujoy Paul, Samet Oymak, and Amit K Roy-Chowdhury. Unsupervised multi-source domain adaptation without access to source data. *arXiv*, 2021. 2, 3, 5, 7
- [2] John S Bridle, Anthony JR Heading, and David JC MacKay. Unsupervised classifiers, mutual information and ‘phantom targets’. 1992. 5
- [3] Zhangjie Cao, Mingsheng Long, Jianmin Wang, and Michael I Jordan. Partial transfer learning with selective adversarial networks. In *Proc. CVPR*, 2018. 2, 8
- [4] Zhangjie Cao, Kaichao You, Mingsheng Long, Jianmin Wang, and Qiang Yang. Learning to transfer examples for partial domain adaptation. In *Proc. CVPR*, 2019. 7, 8
- [5] Nicolas Carion, Francisco Massa, Gabriel Synnaeve, Nicolas Usunier, Alexander Kirillov, and Sergey Zagoruyko. End-to-end object detection with transformers. In *Proc. ECCV*, 2020. 3
- [6] Fabio Maria Carlucci, Lorenzo Porzi, Barbara Caputo, Elisa Ricci, and Samuel Rota Buló. Multidial: Domain alignment layers for (multisource) unsupervised domain adaptation. *IEEE Trans. on PAMI*, 2020. 3
- [7] Mathilde Caron, Hugo Touvron, Ishan Misra, Hervé Jégou, Julien Mairal, Piotr Bojanowski, and Armand Joulin. Emerging properties in self-supervised vision transformers. *arXiv*, 2021. 6
- [8] Jieneng Chen, Yongyi Lu, Qihang Yu, Xiangde Luo, Ehsan Adeli, Yan Wang, Le Lu, Alan L Yuille, and Yuyin Zhou. Transunet: Transformers make strong encoders for medical image segmentation. *arXiv*, 2021. 3
- [9] Xinyang Chen, Sinan Wang, Mingsheng Long, and Jianmin Wang. Transferability vs. discriminability: Batch spectral penalization for adversarial domain adaptation. In *Proc. ICML*, 2019. 3, 7
- [10] Shuhao Cui, Shuhui Wang, Junbao Zhuo, Liang Li, Qingming Huang, and Qi Tian. Towards discriminability and diversity: Batch nuclear-norm maximization under label insufficient situations. In *Proc. CVPR*, 2020. 3, 7
- [11] Shuhao Cui, Shuhui Wang, Junbao Zhuo, Chi Su, Qingming Huang, and Qi Tian. Gradually vanishing bridge for adversarial domain adaptation. In *Proc. CVPR*, 2020. 3, 7
- [12] Jia Deng, Wei Dong, Richard Socher, Li-Jia Li, Kai Li, and Li Fei-Fei. Imagenet: A large-scale hierarchical image database. In *Proc. CVPR*, 2009. 1, 4
- [13] Alexey Dosovitskiy, Lucas Beyer, Alexander Kolesnikov, Dirk Weissenborn, Xiaohua Zhai, Thomas Unterthiner, Mostafa Dehghani, Matthias Minderer, Georg Heigold, Sylvain Gelly, et al. An image is worth 16x16 words: Transformers for image recognition at scale. *Proc. ICLR*, 2021. 2, 3, 4, 5, 7
- [14] Alaaeldin El-Nouby, Natalia Neverova, Ivan Laptev, and Hervé Jégou. Training vision transformers for image retrieval. *arXiv*, 2021. 3
- [15] Yaroslav Ganin, Evgeniya Ustinova, Hana Ajakan, Pascal Germain, Hugo Larochelle, François Laviolette, Mario Marchand, and Victor Lempitsky. Domain-adversarial training of neural networks. *JMLR*. 3, 7, 8
- [16] Jacob Gildenblat and contributors. Pytorch library for cam methods. <https://github.com/jacobgil/pytorch-grad-cam>, 2021. 2
- [17] Ross Girshick. Fast r-cnn. In *Proc. ICCV*, 2015. 1
- [18] Xavier Glorot, Antoine Bordes, and Yoshua Bengio. Domain adaptation for large-scale sentiment classification: A deep learning approach. In *Proc. ICML*, 2011. 1
- [19] Ryan Gomes, Andreas Krause, and Pietro Perona. Discriminative clustering by regularized information maximization. 2010. 5
- [20] Ian J Goodfellow, Jean Pouget-Abadie, Mehdi Mirza, Bing Xu, David Warde-Farley, Sherjil Ozair, Aaron Courville, and Yoshua Bengio. Generative adversarial networks. *Proc. NeurIPS*, 2014. 1
- [21] Xiang Gu, Jian Sun, and Zongben Xu. Spherical space domain adaptation with robust pseudo-label loss. In *Proc. CVPR*, 2020. 7, 8
- [22] Kaiming He, Xiangyu Zhang, Shaoqing Ren, and Jian Sun. Deep residual learning for image recognition. In *Proc. CVPR*, 2016. 1, 4, 5, 7

- [23] Shuting He, Hao Luo, Pichao Wang, Fan Wang, Hao Li, and Wei Jiang. Transreid: Transformer-based object re-identification. *arXiv*, 2021. 3
- [24] Lanqing Hu, Meina Kan, Shiguang Shan, and Xilin Chen. Unsupervised domain adaptation with hierarchical gradient synchronization. In *Proc. CVPR*, 2020. 7, 8
- [25] Weihua Hu, Takeru Miyato, Seiya Tokui, Eiichi Matsumoto, and Masashi Sugiyama. Learning discrete representations via information maximizing self-augmented training. In *Proc. ICML*, 2017. 5
- [26] Lin Huang, Jianchao Tan, Ji Liu, and Junsong Yuan. Hand-transformer: Non-autoregressive structured modeling for 3d hand pose estimation. In *Proc. ECCV*, 2020. 3
- [27] Lin Huang, Jianchao Tan, Jingjing Meng, Ji Liu, and Junsong Yuan. Hot-net: Non-autoregressive transformer for 3d hand-object pose estimation. In *Proc. ACM MM*, 2020. 3
- [28] Sergey Ioffe and Christian Szegedy. Batch normalization: Accelerating deep network training by reducing internal covariate shift. In *Proc. ICML*. PMLR, 2015. 7
- [29] Guoliang Kang, Lu Jiang, Yi Yang, and Alexander G Hauptmann. Contrastive adaptation network for unsupervised domain adaptation. In *Proc. CVPR*, 2019. 1, 3, 7
- [30] Jogendra Nath Kundu, Naveen Venkat, Ambareesh Revanur, R Venkatesh Babu, et al. Towards inheritable models for open-set domain adaptation. In *Proc. CVPR*, 2020. 7, 8
- [31] Vinod Kumar Kurmi, Shanu Kumar, and Vinay P Nambodiri. Attending to discriminative certainty for domain adaptation. In *Proc. CVPR*, 2019. 1
- [32] Chen-Yu Lee, Tanmay Batra, Mohammad Haris Baig, and Daniel Ulbricht. Sliced wasserstein discrepancy for unsupervised domain adaptation. In *Proc. CVPR*, 2019. 1, 8
- [33] Mengxue Li, Yi-Ming Zhai, You-Wei Luo, Peng-Fei Ge, and Chuan-Xian Ren. Enhanced transport distance for unsupervised domain adaptation. In *Proc. CVPR*, 2020. 1, 3, 7
- [34] Rui Li, Qianfen Jiao, Wenming Cao, Hau-San Wong, and Si Wu. Model adaptation: Unsupervised domain adaptation without source data. In *Proc. CVPR*, 2020. 1, 2, 3, 5, 7, 8
- [35] Jian Liang, Dapeng Hu, and Jiashi Feng. Do we really need to access the source data? source hypothesis transfer for unsupervised domain adaptation. In *Proc. ICML*, 2020. 1, 2, 3, 4, 5, 7, 8
- [36] Jian Liang, Yunbo Wang, Dapeng Hu, Ran He, and Jiashi Feng. A balanced and uncertainty-aware approach for partial domain adaptation. *Proc. ECCV*, 2020. 7, 8
- [37] Hong Liu, Zhangjie Cao, Mingsheng Long, Jianmin Wang, and Qiang Yang. Separate to adapt: Open set domain adaptation via progressive separation. In *Proc. CVPR*, 2019. 7, 8
- [38] Jonathan Long, Evan Shelhamer, and Trevor Darrell. Fully convolutional networks for semantic segmentation. In *Proc. CVPR*, 2015. 1
- [39] Mingsheng Long, Yue Cao, Jianmin Wang, and Michael I Jordan. Learning transferable features with deep adaptation networks. *Proc. ICML*, 2015. 1
- [40] Mingsheng Long, Han Zhu, Jianmin Wang, and Michael I Jordan. Unsupervised domain adaptation with residual transfer networks. In *Proc. NeurIPS*, 2016. 1, 3
- [41] Mingsheng Long, Han Zhu, Jianmin Wang, and Michael I Jordan. Deep transfer learning with joint adaptation networks. In *Proc. ICML*, 2017. 1, 3
- [42] Mingsheng Long, Zhangjie Cao, Jianmin Wang, and Michael I Jordan. Conditional adversarial domain adaptation. *Proc. NeurIPS*, 2018. 7, 8
- [43] Zhihe Lu, Yongxin Yang, Xiatian Zhu, Cong Liu, Yi-Zhe Song, and Tao Xiang. Stochastic classifiers for unsupervised domain adaptation. In *Proc. CVPR*, 2020. 8
- [44] Rafael Müller, Simon Kornblith, and Geoffrey Hinton. When does label smoothing help? *arXiv*, 2019. 4
- [45] Daniel Neimark, Omri Bar, Maya Zohar, and Dotan Asselmann. Video transformer network. *arXiv*, 2021. 3
- [46] Pau Panareda Busto and Juergen Gall. Open set domain adaptation. In *Proc. ICCV*, 2017. 2, 8

- [47] Xingchao Peng, Ben Usman, Neela Kaushik, Judy Hoffman, Dequan Wang, and Kate Saenko. Visda: The visual domain adaptation challenge. *arXiv*, 2017. 1, 6
- [48] Fengchun Qiao and Xi Peng. Uncertainty-guided model generalization to unseen domains. In *Proc. CVPR*, 2021. 2
- [49] Fengchun Qiao, Long Zhao, and Xi Peng. Learning to learn single domain generalization. In *Proc. CVPR*, 2020. 2
- [50] Bin Ren, Hao Tang, Fanyang Meng, Runwei Ding, Ling Shao, Philip HS Torr, and Nicu Sebe. Cloth interactive transformer for virtual try-on. *arXiv preprint arXiv:2104.05519*, 2021. 3
- [51] Shaoqing Ren, Kaiming He, Ross Girshick, and Jian Sun. Faster r-cnn: Towards real-time object detection with region proposal networks. *Proc. NeurIPS*, 2015. 1
- [52] Stephan R Richter, Vibhav Vineet, Stefan Roth, and Vladlen Koltun. Playing for data: Ground truth from computer games. In *Proc. ECCV*. Springer, 2016. 1
- [53] Kate Saenko, Brian Kulis, Mario Fritz, and Trevor Darrell. Adapting visual category models to new domains. In *Proc. ECCV*, 2010. 2, 6
- [54] Kuniaki Saito, Kohei Watanabe, Yoshitaka Ushiku, and Tatsuya Harada. Maximum classifier discrepancy for unsupervised domain adaptation. In *Proc. CVPR*, 2018. 1
- [55] Kuniaki Saito, Shohei Yamamoto, Yoshitaka Ushiku, and Tatsuya Harada. Open set domain adaptation by backpropagation. In *Proc. ECCV*, 2018. 7, 8
- [56] Swami Sankaranarayanan, Yogesh Balaji, Carlos D Castillo, and Rama Chellappa. Generate to adapt: Aligning domains using generative adversarial networks. In *Proc. CVPR*, 2018. 1
- [57] Baochen Sun, Jiashi Feng, and Kate Saenko. Return of frustratingly easy domain adaptation. In *Proc. AAAI*, 2016. 1, 3
- [58] Eric Tzeng, Judy Hoffman, Kate Saenko, and Trevor Darrell. Adversarial discriminative domain adaptation. In *Proc. CVPR*, 2017. 1, 3
- [59] Ashish Vaswani, Noam Shazeer, Niki Parmar, Jakob Uszkoreit, Llion Jones, Aidan N Gomez, Lukasz Kaiser, and Illia Polosukhin. Attention is all you need. *arXiv*, 2017. 3, 5
- [60] Hemanth Venkateswara, Jose Eusebio, Shayok Chakraborty, and Sethuraman Panchanathan. Deep hashing network for unsupervised domain adaptation. In *Proc. CVPR*, 2017. 6
- [61] Qiang Wang, Bei Li, Tong Xiao, Jingbo Zhu, Changliang Li, Derek F Wong, and Lidia S Chao. Learning deep transformer models for machine translation. *arXiv*, 2019. 5
- [62] Ximei Wang, Ying Jin, Mingsheng Long, Jianmin Wang, and Michael I Jordan. Transferable normalization: Towards improving transferability of deep neural networks. In *Proc. NeurIPS*, 2019. 3, 7
- [63] Ruijia Xu, Guanbin Li, Jihan Yang, and Liang Lin. Larger norm more transferable: An adaptive feature norm approach for unsupervised domain adaptation. In *Proc. ICCV*, 2019. 7, 8
- [64] Guanglei Yang, Haifeng Xia, Mingli Ding, and Zhengming Ding. Bi-directional generation for unsupervised domain adaptation. In *Proc. AAAI*, 2020. 1, 3, 7
- [65] Guanglei Yang, Hao Tang, Mingli Ding, Nicu Sebe, and Elisa Ricci. Transformers solve the limited receptive field for monocular depth prediction. *arXiv preprint arXiv:2103.12091*, 2021. 3
- [66] Ting Yao, Yingwei Pan, Chong-Wah Ngo, Houqiang Li, and Tao Mei. Semi-supervised domain adaptation with subspace learning for visual recognition. In *Proc. CVPR*, 2015. 1, 3
- [67] Yanhong Zeng, Jianlong Fu, and Hongyang Chao. Learning joint spatial-temporal transformations for video inpainting. In *Proc. ECCV*, 2020. 3
- [68] Jing Zhang, Zewei Ding, Wanqing Li, and Philip Ogunbona. Importance weighted adversarial nets for partial domain adaptation. In *Proc. CVPR*, 2018. 8
- [69] Yang Zhang, Philip David, and Boqing Gong. Curriculum domain adaptation for semantic segmentation of urban scenes. In *Proc. ICCV*, 2017. 1

- [70] Yuchen Zhang, Tianle Liu, Mingsheng Long, and Michael Jordan. Bridging theory and algorithm for domain adaptation. In *Proc. ICML*. PMLR, 2019. 7, 8
- [71] Sixiao Zheng, Jiachen Lu, Hengshuang Zhao, Xiatian Zhu, Zekun Luo, Yabiao Wang, Yanwei Fu, Jianfeng Feng, Tao Xiang, Philip HS Torr, et al. Rethinking semantic segmentation from a sequence-to-sequence perspective with transformers. In *Proc. CVPR*, 2021. 3
- [72] Xizhou Zhu, Weijie Su, Lewei Lu, Bin Li, Xiaogang Wang, and Jifeng Dai. Deformable detr: Deformable transformers for end-to-end object detection. In *Proc. ICLR*, 2021. 3